Thermo-fluid dynamic model of large district heating networks for the analysis of primary energy savings

Elisa, Guelpa; Sciacovelli, Adriano; Vittorio, Verda

DOI:
10.1016/j.energy.2017.07.177

Accepted Manuscript

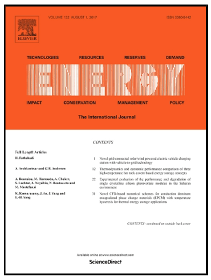

Thermo-fluid dynamic model of large district heating networks for the analysis of primary energy savings

Guelpa Elisa, Sciacovelli Adriano, Verda Vittorio

PII: S0360-5442(17)31372-5

DOI: 10.1016/j.energy.2017.07.177

Reference: EGY 11365

To appear in: *Energy*

Received Date: 10 March 2017

Revised Date: 16 June 2017

Accepted Date: 18 July 2017

Please cite this article as: Guelpa Elisa, Sciacovelli Adriano, Verda Vittorio, Thermo-fluid dynamic model of large district heating networks for the analysis of primary energy savings, *Energy* (2017), doi: 10.1016/j.energy.2017.07.177

Thermo-fluid dynamic model of large district heating networks for the analysis of primary energy savings

Guelpa Elisa[a], Sciacovelli Adriano[b], Verda Vittorio[c]

[a] *Energy Department, Politecnico di Torino, C.so Duca degli Abruzzi 24, 10129 Torino, Italy, elisa.guelpa@polito.it*
[b]*School of Chemical Engineering – Birmingham Centre for Energy Storage (BCES) University of Birmingham, Edgbaston, Birmingham, UK, a.sciacovelli@bham.ac.uk*
[c] *Energy Department, Politecnico di Torino, C.so Duca degli Abruzzi 24, 10129 Torino, Italy, vittorio.verda@polito.it*

ABSTRACT
Among the various heating technologies that can be applied to urban areas district heating is recognized to allow significant reduction in primary energy consumption, provided that the system is properly designed and operated. Thermo-fluid dynamic simulation tools can be of extreme importance in order to achieve this objective. This paper aims at presenting a thermo fluid dynamic model for the detailed simulation of large district heating network and showing how it can be usefully applied to examine options for the reduction of primary energy consumption. The model is tested using experimental data and then applied for analyzing transient operations of the Turin district heating network, which is the largest network in Italy and one of the largest in Europe. A comparison between simulations and experimental results shows that the model is able to predict the temperature in the nodes of the network with good accuracy. The thermal power required to each plant is also calculated with a good level of accuracy. The model can be used for the simulation of operational strategies, thus representing a versatile and important tool for the implementation of advanced management such as the installation of local storage units or the variation of user request schedules.

Keywords:
District heating, Thermal model, Fluid-dynamic model, Network, Optimal management

1. INTRODUCTION

During last decades, district heating (DH) has gained in importance because it allows large-scale integration of waste heat, renewable energies and high efficiency fossil plants for house heating and domestic hot water [1]. The use of centralized power plant allows one to reach high efficiency in particular when a combined production of electrical and thermal energy is performed. Nevertheless, due to the daily and seasonal variation of the demand as well as the availability of the resources, an integration from conventional boilers is often required. In this framework, an important aspect to get efficient district heating systems is the selection of optimal operation and management [2, 3]. Different working conditions should be analysed in order to highlight possible issues and potential improvements associated with technical, economic and environmental reasons. In [4], a review of models to optimize the design of polygeneration systems in district heating network (DHN) is reported. Another important aspect regards the selection of the optimal pumping operations [5] and the maximization of heat production from cogeneration or renewable plants through the modification of the users thermal request [6, 7]. The last point is particularly important in Mediterranean areas, where the morning peak is a typical occurrence, due to the fact that most heating systems are switched off at night. Peak shaving policies are gaining an increasing interest with the goal of decreasing the fraction of heat produced using

boilers and increasing the cogeneration exploitation that leads to an increase in the overall DH system performances.
Investigations on system responses to configuration variations or user request variation can be achieved using models and simulation tools. This is the reason why modelling has been extensively applied to both DH design [8, 9] and management [10, 11]. Regarding DHNs, two main families of approaches can be used for the modelling [12]: black box approaches and physical approaches. In black box approaches, the nonlinearity that characterize the DHN fluid-dynamic problem is overcome using standard transfer functions or neural networks. In order to build and validate these kinds of models, a certain amount of experimental data, or simulation results, are necessary [13, 14]. Physical approaches, instead, rely on mathematical methods for computing mass flows and temperature distributions in the network [15]. Such models need the topological description of the network (pipe lengths, diameters, connections, friction factors), which is usually based on a graph representation of the network. This allows one to obtain a compact definition of the topology, which can be directly used in matrix calculations [16]. Even if these models are more complex and involve larger computational time, they can be used to simulate the DHN behaviour even when significant modifications of the system are operated, e.g. network expansion, failures in pipes, etc.
As far as this second approach is concerned, different types of models have been developed, starting from the pioneering Hardy Cross method [17]. More recently, various models have been proposed in order to overcome the problems related to convergence, computational cost and limitations that affect Hardy Cross method [18]. These methods allow solving the fluid dynamic or the thermal problem and they have been applied to small or medium size networks. Among them it is worth citing the loop equation method [19] (applied to the Zemun supply network with 178 branches, and a length of 4 km), aggregated models [20] (applied to 20 km long network, with 1079 nodes and 10 MW of maximum heat production) and node based model [21]. Both aggregated and node-based models do not solve fluid-dynamic and thermal transient conservation equations within all the nodes of the network [22]. Stevanovic et al. 2009 [22] have solved the thermo-fluid dynamic problem of the Zemun network, neglecting heat losses. In Ben Hassin and Eicker 2011 [23] a model has been designed for the hydraulic and thermal simulation of DHN and applied to the DH network in Scharnhauser Park which is a network with 584 consumers and a total length of about 13.5 km. In both these works no information about computational costs are provided. Computational cost is an important characteristics of a DHN simulation tool for management analysis, in particular when large systems are considered. In fact there are many large district heating networks, which detailed representation involves a high number of nodes and branches. Solution of both the fluid-dynamic and thermal problems may require very high computational resources, therefore an alternative approach has to be used in these cases. In particular a suitable model strategy is required when optimization in transient conditions are requested.

This paper presents a new method for solving both thermal and hydraulic problems while analyzing large district heating systems, also involving loops. The model is used to solve separately the transportation network and the distribution networks in order to make the computational cost acceptable. The model capability to reproduce network behavior is tested through some experimental data collected in the Turin district heating system, the largest in Italy, being more than 2500 km long and connecting more than 5500 buildings. Its graph representation is based on more than 60000 nodes. The model predicts the evolution of heat load required during the daily transient. Numerical results are compared with real data.
The main novelty of this work is the possibility of obtaining the evolution of the thermal-fluid dynamic quantities in all the nodes of a large DHN through a very fast model. ~~This work~~ It provides the basis for a complete operational optimization, in particular for the optimal exploitation of power plants, storage systems and DHN water pumping system. In this paper it is applied to peak shaving the thermal load of the plants in order to minimize primary energy consumption through optimal schedule of the building requests.

2. THE THERMO-FLUID DYNAMIC MODEL

In this section the model used for solving the fluid-dynamic and thermal problems of large district heating networks is described. This is based on a one dimensional formulation of the conservation equation (continuity, momentum, energy). The topology of the network is described using a graph approach [16]. Each pipe is considered as a branch delimited by two nodes, which are identified as the inlet node and outlet node on the basis of a reference direction (velocity is positive when the fluid is flowing in the same direction as the reference direction and negative when flowing in the opposite direction). The incidence matrix, A, is used to express the connections between nodes and branches. Matrix A has as many rows as the number of nodes and as many columns as the number of branches. Its general element A_{ij} is equal to 1 or -1 if the branch j enters or exits the node i and 0 otherwise.

The fluid-dynamic model considers the mass conservation equation applied to all nodes and the momentum equation to all branches. In the fluid-dynamic model, a series of hypotheses are considered:

- The unsteady term is not considered since fluid-dynamic perturbations travel the entire network in a period of time of few seconds, smaller than the time steps adopted for calculations (usually >60 s).
- Density is considered as constant, which also means that the velocity changes between the inlet and the outlet of a branch are assumed as negligible.

The mass balance of a node can be written as:

$$\sum G_{in} - \sum G_{out} = \mathrm{G}_{ext} \tag{1}$$

where G_{in} are the mass flow rates entering the nodes from the upstream branches, G_{out} the mass flow rates exiting the node and entering the downstream branches and G_{ext} a mass flow rate exiting outwards.

The mass balance equation can be written for the entire network using matrix formulation:

$$\mathbf{A} \cdot \mathbf{G} + \mathbf{G_{ext}} = 0 \tag{2}$$

where **G** is the vector containing the mass flow rates in the branches and $\mathbf{G_{ext}}$ the vector that contains the mass flow rates exiting or exiting the nodes outwards. The terms in $\mathbf{G_{ext}}$ are different than zero in the case of open networks, i.e. when only a portion of the entire closed circuit is considered (e.g. only the supply or the return network as often considered in the analysis [24]). In particular, $\mathbf{G_{ext}}$ is positive when the mass flow rate enters the network and negative when it exits.

The steady-state momentum equation in a branch for an incompressible fluid is written adding the gravitational term to the static pressure:

$$\left(\mathrm{p_{in}} - \mathrm{p_{out}}\right) = \frac{1}{2}\frac{\mathrm{f}}{\mathrm{D}}\mathrm{L}\frac{\mathrm{G}\,|\mathrm{G}|}{\rho \mathrm{S}^2} + \frac{1}{2}\sum_{\mathrm{k}}\beta_{\mathrm{k}}\frac{\mathrm{G}\,|\mathrm{G}|}{\rho \mathrm{S}^2} - \tau \tag{3}$$

where p is the total pressure, while the first and the second terms on the right-hand side terms are the distributed and the localized pressure losses, and the last term is the pressure rise due to the pumps that may be located in the branch. Equation (3) can be rewritten as:

$$\mathrm{G} = \mathrm{Y}\left(\mathrm{p_{in}} - \mathrm{p_{out}}\right) + \mathrm{Y}\tau \tag{4}$$

where the term Y is the fluid dynamic conductance of the branch, expressed as:

$$\mathrm{Y} = \mathrm{r}^{-1} = \left[\frac{1}{2}\frac{\mathrm{G}}{\rho \mathrm{S}^2}\left(\frac{\mathrm{f}}{\mathrm{D}}\mathrm{L} + \sum_{\mathrm{k}}\beta_{\mathrm{k}}\right)\right]^{-1} \tag{5}$$

The friction factor f has been evaluated using an explicit Haaland correlation [25] in order to avoid iterative calculations and thus reduce the computational cost of the simulations.

Momentum equation can be rewritten in matrix form. This formulation is obtained using the incidence matrix and relate the quantities that are defined at the branches (mass flow rates and pressure variations due to friction and pumping) with pressures at the inlet and outlet nodes:

$$\mathbf{G} = \mathbf{Y} \cdot \mathbf{A}^{\mathrm{T}} \cdot \mathbf{P} + \mathbf{Y} \cdot \boldsymbol{\tau} \qquad (6)$$

The diagonal matrix $\mathbf{Y}$ contains the fluid dynamic conductance of branches. Because of the dependence of $\mathbf{Y}$ on the mass flow rates, the system of equations is non-linear. Equation (6) is finally modified by setting proper boundary conditions. At least one pressure should be set in a boundary node. In the case of analyses applied to a closed network, pressure is set on the node representing the pressurization system. In the case only supply or return networkis analyzed, i.e. an open network, pressure is usually set at the master thermal plant. Boundary conditions involving mass flow rates at the nodes ($\mathbf{G_{ext}}$) are usually expressed when a portion of the network is analyzed. These are imposed at the nodes representing the users and, in the case of multiple plants, at nodes associated with the slave plants.

Because of the non-linearity of Eq. 6 and the coupling between mass and momentum equations, the problem requires an iterative algorithm. The SIMPLE (semi implicit method for pressure linked equation) algorithm [26] has proven to be efficiently applied to this purpose especially in the case of networks with multiple loops and booster pumps. This is a guess and correction method: a pressure vector $\mathbf{P'}$ is first guessed and during the iterations it is corrected together with the mass flow rate vector obtained using (6). Through the initialization $\mathbf{P}$=$\mathbf{P'}$ it is possible to evaluate $\mathbf{G'}$as

$$\mathbf{G'} = \mathbf{Y'} \cdot \mathbf{A}^{\mathrm{T}} \cdot \mathbf{P'} + \mathbf{Y'} \cdot \boldsymbol{\tau} \qquad (7)$$

where $\mathbf{Y'}$ is built considering $\mathbf{P}$ =$\mathbf{P'}$ and an initial guess of mass flow rate $\mathbf{G_0}'$. Eq. (7) is nonlinear, therefore a proper algorithm has to be used for its solution such as the fixed point algorithm [27]. The correction of the mass flow $\boldsymbol{G_{corr}}$ rate and the pressure $\boldsymbol{P_{corr}}$ are defined as:

$$\boldsymbol{P} = \mathbf{P'} + \boldsymbol{P_{corr}} \qquad (8)$$

$$\boldsymbol{G} = \mathbf{G'} + \boldsymbol{G_{corr}} \qquad (9)$$

Combining together equations (6) and (7) it is possible to obtain:

$$\mathbf{G} - \mathbf{G'} = \mathbf{Y} \cdot \mathbf{A}^{\mathrm{T}} \cdot \mathbf{P} - \mathbf{Y'} \cdot \mathbf{A}^{\mathrm{T}} \cdot \mathbf{P'} + (\mathbf{Y} - \mathbf{Y'}) \cdot \boldsymbol{\tau} \qquad (10)$$

which becomes:

$$\boldsymbol{G_{corr}} = \mathbf{Y} \cdot \mathbf{A}^{\mathrm{T}} \cdot \boldsymbol{P_{corr}} \qquad (11)$$

under the assumption of ($\mathbf{Y} = \boldsymbol{Y}'$). Substituting Eq. (9) into Eq. (2) it is possible to obtain Eq. (12).

$$\mathbf{A} \cdot \boldsymbol{G_{corr}} = -\mathbf{A} \cdot \mathbf{G'} - \mathbf{G}_{\mathrm{ext}} \qquad (12)$$

The substitution of (11) in (12), allows one to write Eq. (12) as follows:

$$\mathbf{A} \cdot \mathbf{Y'} \cdot \mathbf{A}^{\mathrm{T}} \cdot \boldsymbol{P_{corr}} = -\mathbf{A} \cdot \mathbf{G'} - \mathbf{G}_{\mathrm{ext}} \qquad (13)$$

which can be rewritten in a simpler form:

$$\boldsymbol{H} \cdot \boldsymbol{P_{corr}} = \boldsymbol{d} \qquad (14)$$

considering:

$$\mathbf{H} = \mathbf{A} \cdot \mathbf{Y'} \cdot \mathbf{A}^{\mathrm{T}} \qquad (15)$$

$$\mathbf{d} = -\mathbf{A} \cdot \mathbf{G}' - \mathbf{G}_{\text{ext}} \tag{16}$$

Eq. (14) can be used to evaluate the pressure correction $\mathbf{P_{corr}}$, while it is possible to evaluate **P** through Eq. (8). Furthermore, **G** can be obtained by using Eq. (11) and Eq. (9). **P** and **G** can thus be used as new guess values for the following iteration. The procedure is carried out until the convergence is reached. In order to evaluate the convergence level, residuals can be calculated through Eq. 17 and 18; the convergence is reached when the values R1 and R2 are both lower than the tolerance value. In this case a tolerance value of 0.001 is selected.

$$\mathbf{G}' - \mathbf{Y}' \cdot \mathbf{A}^{\mathrm{T}} \cdot \mathbf{P}' - \mathbf{Y}' \cdot \boldsymbol{\tau} = \boldsymbol{R_1} \tag{17}$$

$$\mathbf{A} \cdot \mathbf{G} - \mathbf{G}_{\text{ext}} = \boldsymbol{R_2} \tag{18}$$

To improve the process of convergence, an under relaxation factor (α) can be used while updating pressures and mass flow rates, therefore Eq. (8) and Eq. (9) become:

$$\boldsymbol{P} = \mathbf{P}' + \alpha \boldsymbol{P_{corr}} \tag{19}$$

$$\boldsymbol{G} = \mathbf{G}' + \alpha \boldsymbol{G_{corr}} \tag{20}$$

As regards boundary conditions, the mass flow rates entering and exiting the system are directly set in the vector $\mathbf{G}_{\text{ext}}$. To express pressures in nodes (at least one), the boundary value is imposed in the initial guess vector **P'**; furthermore, no correction is applied on it in order to keep it fixed. This means that matrix **H** should be modified so that, the row related to the node where pressure is imposed, present all zeros except for the value in the diagonal term which is 1, while vector **d** is zero in the corresponding row.

A schematic of the SIMPLE procedure is depicted in Figure 1. Further details can be found in [28].

The thermal model is based on the energy equation applied to all the nodes of the network. The control volume considered for the analysis is reported in Figure 2.

This includes the junction, node and half of each duct entering or exiting the junction. Adiabatic and perfect mixing is assumed, such that the temperature of water exiting the i^{th} node through each of the j branches is at the same temperature while heat losses are ascribed to the branches. The energy conservation equation for the i^{th} node, considering negligible both the compressibility effects and the viscous heating, can be written as:

$$\rho\, c \frac{\partial T}{\partial t} + \rho\; c\, v \cdot \nabla T = \nabla \cdot k \nabla \mathrm{T} + \varphi \tag{21}$$

where the first term is the transient term, the second term represents the contribution due to mass flow rates in all the branches connected to the i^{th} node, the first right-hand side term is the conductive term and the last one contains the contribution of thermal source and losses.

The energy equation is expressed in transient form for two main reasons:

1. A network, especially in the case it is large, may be is characterized by a very large heat capacity.
2. Thermal perturbations travel the network at the water velocity, which is of the order of few meters per second i.e. much smaller than pressure perturbations; velocity depends on the request and the portion of network, being typically small at night and in the distribution networks i.e. closer to the users. Temperature variations may thus take a lot of time to reach the thermal plants.
   Both these phenomena make the thermal load of the plants at a specific time different than the summation of the thermal request of buildings.

Neglecting the contribution of the conduction heat in the fluid along the network and considering the problem as one dimensional we obtain:

$$\frac{\partial(\rho\, c\, T)}{\partial t} + \frac{\partial(\rho\, c\, v\, T)}{\partial x} = \varphi \qquad (22)$$

Integrating Eq. (22) it is possible to obtain:

$$\frac{\partial(\rho c T)_i}{\partial t}\Delta V_i + \sum_j c G_j T_j = U\,(T_i - T_{env}) \qquad (23)$$

where the thermal losses have been expressed as the product of the global heat exchange coefficient U and the temperature difference between the water in the pipe and the temperature of the ground around the pipe. The fact that the control volume shown in Figure 2 is considered implies that heat losses are calculated on the basis of temperature in the nodes. In the case large temperature decrease occurs between consecutive nodes occurs, a better approximation of heat losses can be obtained using additional nodes, which have a numerical role only.

In order to relate branches and nodes an Upwind scheme [29], that assigns to the j^{th} branch the temperature of the previous node considering the actual fluid flow direction, is used. Equation (23) can be written in matrix form for all nodes:

$$\mathbf{M} \cdot \dot{\mathbf{T}} + \mathbf{K} \cdot \mathbf{T} = \mathbf{g}\,, \qquad (24)$$

where **M** is the mass matrix, a diagonal matrix which contains the coefficients ($\rho c \Delta V_i$) of the dynamic term, **K** is the stiffness matrix, which includes the coefficients of the term linearly dependent on temperature, and **g** is the vector containing the known quantities. Dirichlet boundary conditions (i.e. node at imposed temperature) are imposed in all the inlet nodes connected to a single pipe. In the case the inlet node is connected to more than one pipe, the mass flow rates generally mix together, therefore the node temperature cannot be imposed. An inlet mass flow rate with prescribed temperature is imposed instead. In the case of a close network, temperature should be fixed in the node representing the pressurizing system.The whole procedure used in order to evaluate the mass flow rate evolution and the temperature evolution is reported in Figure 3.

In Figure 4, the time required to solve a single iteration of the thermo-fluid dynamic model is reported as a function of number of nodes. Calculations have been performed implementing the code in Matlab® and using a single 3.3 GHz CPU. If the number of nodes becomes large, the computational cost dramatically increases, due to the necessity to solve the conservation equations in all the nodes and branches. The mathematical relation between the nodes and branches in a network is expressed through the Euler's formula, reported in (25) for a single network:

$$l = n - b + 1 \qquad (25)$$

where l is the number of loops, n the number of nodes and b the number of branches. As the number of loops is generally limited compared with the number of nodes, results reported in Figure 4 do not significantly depend on the number of loops. The deviation among the evolution obtained considering a looped network respect to a tree shaped network is of the order of 3%. In the case of large networks, a possible approach to speed up the calculation consists in solving the transport network and distribution networks separately. An example of such approach is considered in next sections.

The total heat load required to the network is computed using the energy equation at the thermal plants, which can be expressed as:

$$\Phi = \sum_i G_{RET_i} c\,(T_{SUP} - T_{RET_i}) \qquad (26)$$

where, G_{RETi} is the mass flow rate that enters (and exits) the i^{th} plant ,T_{SUP} is the water temperature at the outlet of the power plants (supply pipeline), T_{RETi} is the water temperature at the inlet of the i^{th} plant (return pipeline) and c the specific heat. Mass flow rates at the various buildings are set as boundary conditions on the supply and return networks. The mass flow rate entering the various power plants, G_{RETi}, is a consequence of the request of the buildings and is adjusted in order to comply with the inlet point temperature on the secondary side. Simulation of supply network allows one calculating the inlet temperature at each building, i.e. in the open nodes where water exits the supply network. Water exiting the heat exchangers in the buildings flows in the return network and mixes with the streams coming from the various buildings. Streams exiting the distribution networks are at different temperatures, due to the different distance of the distribution networks from the plants. In the end, temperature evolution at the plant is significantly different than that at the users. The present model is used for determining the temperature evolution at the plants T_{RETi}, starting from information at the buildings, which is crucial to investigate possible effects of actions operated at the buildings or at the thermal plants, as described in the last section.

3. APPLICATION

The thermo-fluid dynamic model for district heating networks is here applied to the Turin district heating network, which is the largest network in Italy and one of the largest in Europe. This application has been used in order to show the model capability to analyze large networks in details. The system supplies heat to about 5500 buildings with a total volume of 56 million m^3. The annual thermal request is about 2000 GWh and the maximum thermal power request is over 1.3 GW. The network is about 2500 km long and its full representation requires more than 60000 nodes.

Heating is produced in six thermal plants located in different areas of the network. There are 3 cogeneration groups, 5 groups of boiler systems and 3 groups of storage tanks, located in different areas of the network. The storage capacities are 5000 m^2 for Torino Nord (6 units) and 2500 m^2 for Martinetto (3 units) and Politecnico (3 units). Their thermal power have been evaluated considering a typical temperature difference between the supply and the return and the maximum water mass flow rate which is supplied and extracted at the storage tanks. The latter has been obtained on the basis of the storage volume and the usual discharging time.

A description of the configuration of the plants with their characteristics is provided in Table 1. The water supply temperature is kept almost constant to about 120°C during winter season while the return temperature varies depending on the total thermal load.

As already mentioned the entire network can be considered as composed of two parts: a transportation network and a distribution network. The transportation network consists in large diameter pipes, usually larger than 200 mm. It is 140 km long and includes 1373 nodes and 1389 branches and 17 loops. This configuration, with multiple loops, is used to limit possible effects of failures as well as to allow better flow distribution. It connects the thermal plants to each distribution network through a node called barycentre. A distribution network supplies water to groups of buildings that are located in the same area. From the fluid-dynamic point of view, the transportation network and distribution networks are a unique network. Barycentres are the nodes where the distribution networks are connected with the transportation network. The separation has been performed with the aim of reducing the computational time required to solve the whole network.

In the Turin network there are 182 distribution networks. The distribution networks are generally tree-shaped networks but some of them also present loops. Figure 5 depicts the transportation pipeline network and, in detail, 3 distribution networks.

The barycentres related to the 3 reported distribution networks are called S1, S2, S3. The 3 selected distribution networks are characterized by a very different number of buildings connected. In particular S1 is a large distribution network (>100 users), S2 is a small distribution network (<30 users) and S3 is a medium size distribution network.

All the users are connected to the distribution network through heat exchangers. Most of the heat exchangers in the distribution networks are equipped with a flow meter on the primary sides. The inlet and outlet temperatures on the primary side (the distribution network side) and the temperature of water supplied to the building heating systems are also monitored. Data are provided each 6 minutes. This piece of information allows to know the evolution of the heat exchanged at each building and is used here for validating the model.

The buildings that are specifically analyzed in the present work are also reported in Figure 5; they are located in the distribution network linked to the barycentre S1 and are indicated U1, U2, U3, U4. These buildings are characterized by different volume, with a consequent different thermal request. The start-up time of their heating systems changes between 3.30 a.m. and 6.30 a.m. Furthermore the heating schedules are different; two of them are always on during the day and they are switched off only during the night, while the others are switched off one or more times also during the day. In Table 2 the time schedules of the heating system of the four buildings are detailed.
The model described in the previous section can be used in order to simulate the behavior of the whole network. The mass flow rates at each substation available from measurements cannot be imposed as boundary conditions in the simulation but are obtained through iterative adjustments of the valves. This approach has been used in [5, 13, 30] in order to simulate the main pipeline of the Turin district heating network.
In this work the transportation network and all the distribution networks of the Turin district heating system are considered: first the transportation network of the supply pipeline is simulated (Figure 6a) and then the results obtained are used as boundary conditions to the distribution pipelines (Figure 6b). As regards the return pipeline, first the distribution networks are simulated (Figure 6c) and the results are used as boundary conditions to the transportation pipeline (Figure 6d).

4 RESULTS

The network model provides values of pressure and temperature in each node and mass flow rate in each branch. The analysis is here applied to the transient operation in a specific period of year having in mind different objectives:

- validate the proposed model;
- show the information that can be gained from the model
- help discussing possible applications of the model

The validation of the model has been carried out comparing the calculated and measured values of temperature in some nodes of the distribution network and also the heat fluxes exchanged at the various plants. In particular, the temperatures at the inlet section of the heat exchangers, measured on the primary side of the heat exchangers of users U1, U2, U3, U4, shown in Figure 5 are examined. The temperature evolutions obtained with the model are compared with the experimental data in Figure 7. For each building, the evolution of the corresponding mass flow rate entering the heat exchanger is also appended in order to clarify the system behaviour. During transient, the temperature at the inlet section of user mass flow rate is not constant: at night temperature drops in all the heat exchangers due to the very low mass flow rate in the pipeline (see figure 6 on the right) and the almost constant heat losses. This also means that the ratio between heat transportation and heat losses decreases. During the day, the temperature evolutions present different peculiarities, depending on the heating strategy adopted by the users. In the case of the buildings U1 and U2, temperature is almost constant during the day due to the fact that the system is not stopped. In these figures it is possible to notice that a peak request occurs when the system is switched on. This is related with the decrease in the temperature of the local heating circuit (secondary side) taking place at night. When the system is switched on, the heat flux exchanged at the heat exchanger is much larger than the design value because of the very large temperature difference between primary and secondary sides. System U3 is switched off twice during the day and system U4 once. This can be clearly noticed from the mass flow rate evolution. Each time the system is switched on, the mass flow rate presents a peak even if this is much smaller than that occurring after night. This is because the temperature decrease at the secondary side during the pauses is limited. The comparison between model results and experimental data demonstrates that the model is able to reproduce the daily temperature evolution in the points of the considered network with sufficient accuracy. The mean relative error is lower than 10%. In particular, the model correctly detects the temperature when the heating system is operating. In this phase, the mean relative error drops to less than 2%. Also during the network cooling transient the model simulates properly the temperature reduction, even if the reduction takes place slower. This is mainly due to the heat losses of the thermal substations, which are not considered in the model but are relevant in percentage during stops. This phenomenon is even more evident when systems are stopped during the day: the model detects the temperature reduction but the trend in simulations shows a much slower decrease with respect to the experimental data, especially for building U3.

The return distribution networks have been analyzed to obtain the thermal load evolution. Temperatures of the fluid exiting the various heat exchangers have been set as the boundary conditions for the thermal problem. As a result, the temperature at the nodes connecting the distribution networks at the main pipeline are obtained. The thermal request to the 3 distribution networks can thus be obtained. The requests of distribution networks S1, S2, S3 are reported in Figure 8.

In general, the thermal load is quite constant during the last hours of the evening, then it dramatically decreases at 11 p.m. and remains about constant, during the night. These values do not go to zero because some of the connected users require thermal power also during the night. Early in the morning the mass flow rate gradually increases between 5 a.m. and 6.30 a.m. in order to fulfill the start-up requirements. Then it decreases and remains about constant between 8 am and 10 am.

Thermal requests in these networks are very different. This result suggests that the distribution networks cannot be just analyzed as if they were all similar, but the specific behaviour in terms of different thermal capacity and schedules of the various buildings should be considered, particularly when the goal of the model consists in implementing energy saving strategies at a building level. A detailed analysis shows that both the maximum peaks (2704 MW, 309 MW, 172 MW) and the ratio between the peak amplitude and the off peak request, i.e. pseudo steady state request, are quite different. The peak amplitude is evaluated as the difference between the maximum peak and the off peak request. For S1, S2 and S3, the computed ratio between the peak amplitude and the off-peak request are 0.84, 0.87 and 0.80, respectively. No relation to the network size is observed. The ratio between the peak and the night request is quite similar: 0.957, 0.959, 0.969 respectively. The duration of peaks are between 60 and 75 minutes and the shape is very different.

The heat load required to the thermal plants are calculated in order to evaluate the performance indication of the system. Results are reported in Figure 9. In the examined scenario, which corresponds to a cold day of April, the base thermal power is mainly provided to the Torino Nord power plant, which is a cogeneration power plant. The other cogeneration plant, i.e. Moncalieri power plant, is used only during the start-up transient, in the morning. The energy storage units provide heat in the evening and during the morning peak, while during night they are charged, as shown to the negative values in Figure 9. The Bit power plant is not used. Comparison with measurements shows that the mean error is lower than 10%, and much lower (about 7%) for the storage systems. The model is able to predict with a good level of accuracy the thermal load required to each thermal plant.

The evolution of total thermal load during the transient between 7.00 p.m. and 10.00 a.m. is reported in Figure 10. During the evening, the load is almost constant to about 330 MW. In this part the model slightly overestimates the request, mainly due to the small variations in the supply temperature. During the night, the load reduces to about 70 MW and remains almost constant until early morning. In this portion of curve the model is able to simulate real data with good accuracy. The energy demand reaches the maximum value of about 800 MW during start-up, at 6.45 a.m. After that the heat required slightly decreases until a value of about 450 MW.

The thermo-fluid dynamic model is able to predict the peak load position and the requested thermal power. The mean relative error during the stationary thermal request and the peak request is about 5%. However, the small differences occurring between real and simulated power evolution are mainly due to the supply temperature changes as well as on the fact that the data registered by the monitoring system refer to about 50% of the connected buildings, therefore the lacking data have been obtained through extrapolation.

The results provided to the model could be used to predict the thermal power demand and peak load position with different load conditions in order to implements primary energy saving plans strategies.

The computational time needed to solve the thermo-fluid dynamic model for the entire 15 hour transient considering the whole network is about 2 hours on a single 3.3 GHz CPU. Therefore this model can be used in order to simulate large district heating networks with an appreciably low computational cost. In particular it is a very satisfactory result when compared to value of computational cost needed for one iteration of the fluid dynamic model if the network was considered as a single system, which is about 22 hours.

5 DISCUSSION

The physical simulation tool proposed in the previous sections can be applied to large DH networks to obtain information for optimizing operations and management. Knowledge of the evolution of network variables as the function of time in each node is very useful for different reasons.

One of the most important aspects that can be analyzed is the possibility of thermal load peak shaving. The model can thus be applied for analyzing the effect on the thermal request due to the application of virtual storages or the installation of distributed or decentralized storage tanks. A virtual thermal storage consists intaking advantage of the thermal capacity of the building. The thermal request profiles of some of the buildings connected to a DH network can be modified with the aim of obtaining a peak reduction thermal load. An effective application of virtual storages is possible only if the effect of possible changes in user thermal demand on the global thermal load are known. Knowledge of such relation it is possible through a detailed thermo-fluid dynamic model of the district heating network, able to simulate the temperature and mass flow rate evolution along the network. In Guelpa *et al.* 2016 [31] the model has been applied to a distribution network in order to find the optimal start-up strategy for the minimization of the primary energy consumption and the thermal peak. Results show that without simulation of the network such evaluation would not be correct because of the time delays, mixing effects and the thermal capacity associated with the pipeline.

In order to perform this kind of analysis a model of the heating system of buildings has to be included. A compact model able to simulate both the substation and the heating system has already been designed and implemented. The substation device is modeled trough a heat exchanger, where district heating network water flows on the primary side and the building heating fluid on the secondary side. The heating system is simulated trough a second, fictitious, heat exchanger, linked on one side with the building heating fluid while on the other side it exchanges heat with the indoor environments. The heat exchangers are modeled using a effectiveness-NTU method. Between the two heat exchangers, a certain time delay is considered for accounting for the average time requested for water circulation on the secondary network. For detail see Verda *et al.*2016 [32].

The effect of the installation of storage systems on the network should also being examined considering the network model. The reduction of the thermal peak and the consequent primary energy savings can be evaluated for different storage sizes. It is possible to evaluate the best storage volume or position that allow to minimize the primary energy consumption. As an example, the model here has been used to analyze the effects of the future network expansions with and without storages installation. Such expansion in the case of the Turin network has been already planned. In particular the area to be connected is located in a portion of the network characterized by a large energy demand and water velocity and the pipeline is close to the upper limit when a large request is considered. The storage tanks are supposed to be charged between 4.30 am and 5.30 am. In Figure 11a a comparison with and without storages is shown; Figure 11b just shows the peak in details. The presence of the storages induces an increase in thermal request between 4.30 am and 5.30 am and a remarkable reduction of the peak thermal load. This allows the use of the cogeneration plants for a larger fraction of the thermal request. In fact the peak shaving induces a lower use of boiler with a consequent primary energy saving. In particular the maximum peak is reduced of about 60 MW. The total energy amount removed to the peak due to the storages installation, in the day considered, is about 25 MWh. In addition, the maximum mass flow rate in the portion of pipeline towards the area to be connected is kept below the maximum limit.

The model can also be used with the aim of simulating the effects of alternative approaches for adjusting the thermal request. An important aspect for operation management is the evaluation of the effects of the supply temperature changes in the global thermal demand with the aim of quantifying the potential on primary energy consumption. In particular the integration of lower temperature resources, such as waste heat from industrial sites or renewable sources can be analyzed [33].

6 CONCLUSIONS

This paper presents a transient thermo-fluid dynamic model of large district heating networks, that can be used for peak shaving analysis. The model has been applied to the largest district heating network in Italy, located in Turin, for the analysis of morning start-up operation.

The model is based on a steady state fluid-dynamic model and a transient thermal model of the network. The fluid-dynamic model evaluates the mass flow rates in branches and pressures in nodes using the SIMPLE algorithm. The thermal model determines the temperature in the nodes using an Upwind scheme. The model has been applied to the transportation network as well as to distribution networks. In order to keep computational cost low, the proposed method can be used through a particular approach: the transportation and distribution networks are simulated separately, through the implementation of a boundary condition cascade which transfers information from each portion to the next.

The approach used in this work allows one to reduce the time required for simulation of 4 order of magnitude with respect to the full network at once. Simulation of 15 hour operation for the whole network (supply line only) on a single 3.3 GHz CPU is about 2 hours. This is a reasonable amount for a large district heating network.

Data calculated at each time step in all branches and nodes offer the opportunity to perform analysis at different levels of the network. The temperatures in various nodes of the network have been compared with experimental data to prove the model effectiveness. Results of this comparison shows that the temperature evolution during the whole day is predicted accurately. Furthermore, the model allows obtaining the thermal power required to each of the plants supplying heat to the network. The total thermal request is also evaluated with a good level of approximation: the average error is about 5%. This is a useful decisional support in operational strategies, such as the evaluation of electricity production by the cogeneration systems, the analysis of thermal peak shaving that can be obtained by installing storage systems, as well as the promotion of night attenuation or variations in the thermal request profile of the users. The present tool allows one obtaining these results with low computational cost, even in the case of large DHNs.

ACKNOWLEDGEMENTS
Authors are very grateful to the technicians of IREN for providing the operation data used in this work.

REFERENCES

[1] Lund H, Moller B, Mathiesen BV, Dyrelund A. The role of district heating in future renewable energy systems. Energy 2010; 35: 1381–1390.

[2] Casisi M, Pinamonti, P, Reini M. Optimal layout and operation of combined heat & power (CHP) distributed generation systems. Energy 2009; 34(12): 2175-2183.

[3] Aringhieri R, Malucelli F. Optimal operations management and network planning of a district heating system with a combined heat and power plant. Annals of Operations Research 2003; 120(1-4): 173-199.

[4] Ortiga, J, Bruno, JC, Coronas, A, Grossman, IE. Review of optimization models for the design of polygeneration systems in district heating and cooling networks. Computer Aided Chemical Engineering 2007; 24: 1121-1126.

[5] Sciacovelli A, Guelpa E, Verda V. Pumping cost minimization in an existing district heating network. Proceedings of IMECE;2013 November15-21; San Diego, California, USA.

[6] Verda V, Baccino G. Primary energy reductions in District Heating Networks through variation of the thermal load profile of the users. Proceedings of ECOS 2014. Turku, Finland, June 15-19.

[7] Jokinen E, Kontu K, Rinne S, Lahdelma R. Demand side management in District Heating buildings to optimize the heat production. Proceedings of ECOS 2014. Turku, Finland, June 15-19.

[8] Dalla Rosa A, Li H, Svendsen S. Method for optimal design of pipes for low-energy district heating, with focus on heat losses. Energy 2011; 36(5): 2407-2418.

[9] Ancona MA, Melino F, PerettoA. An Optimization Procedure for District Heating Networks. Energy Procedia 2014; 61: 278-281.

[10] Li L, Zaheeruddin M. A control strategy for energy optimal operation of a direct district heating system. International Journal of energy research 2004; 28(7): 597-612.

[11] Bojic M, Trifunovic N. Linear programming optimization of heat distribution in a district-heating system by valve adjustments and substation retrofit. Building and Environment 2000; 35: 151-159.

[12] Larsen HV, Pálsson H, Bøhm B, Ravn, HF. Aggregated dynamic simulation model of district heating networks. Energy conversion and management 2002;*43*(8): 995-1019.

[13] Guelpa E, Toro, C, Sciacovelli A, Melli R, Sciubba E, Verda, V. Optimal operation of large district heating networks through fast fluid-dynamic simulation. Energy 2016; 102: 586-595.

[14] Keçebaş A, Yabanova İ. Thermal monitoring and optimization of geothermal district heating systems using artificial neural network: A case study. Energy and Buildings 2012; 50: 339-346.

[15] Palsson H, Methods for Planning and Operating Decentralized Combined Heat and Power Plants, R&J National Laboratory, Roskilde Denmark; 2000; Report 1185.

[16] Harary F, Graph Theory. Narosa Publishing House, New Delhi; 1995.

[17]Cross H. Analysis of flow in networks of conduits or conductors. EngExp Station 1936; 286: 3–29;

[18] Lindell E Ormsbee, The History of water distribution Network Analysis: The Computer Age. Proceedings of Water Distribution Systems Analysis Symposium; 2006 August 27-30; Cincinnati, Ohio, USA.

[19] Stevanovic VD, Prica S, Maslovaric B, Zivkovic B, Nikodijevic S. Efficient numerical method for district heating system hydraulics. Energy Conversion and Management 2007; 48: 1536–1543.

[20] Larsen HV, Palsson H, Bøhm B, Ravn HF. Aggregated dynamic simulation model of district heating networks. Energy Conversion and Management 2002; 43: 995–1019.

[21] Benonysson A, Bohm B, Ravn HF. Operational optimization in a district heating system. Energy Conversion and Management 1995; 36: 297-314.

[22] Stevanovic VD, Zivkovic B, Prica S, Maslovaric B, Karamarkovic V, Trkulja V. Prediction of thermal transients in district heating systems. Energy Conversion and Management 2009; 50: 2167–2173.

[23] Hassine IB, Eicker U. Simulation and optimization of the district heating network in Scharnhauser Park. In Proceedings of 2ndPolygeneration Conference (2nd ECP), 2011Tarragona (Vol. 30, pp. 2011-1).

[24] Fang T, Lahdelma R. State estimation of district heating network based on customer measurements. Applied Thermal Engineering 2014; 73(1): 1211-1221.

[25] Haaland SE. Simple and Explicit Formulas for the Friction Factor in Turbulent Flow. Journal of Fluids Engineering 1983; 103 (5): 89–90.

[26] Patankar SV. Numerical Heat Transfer and Fluid Flow;1980.

[27] Lefschetz S. On the fixed point formula. Annals of Mathematics 1937; 819-822.

[28] Sciacovelli A, Verda V, Borchiellini R, Numerical Design of Thermal Systems. Clut, Torino; 2015

[29] Peric M, &Ferziger JH. Computational methods for fluid dynamics. 1996

[30] Cosentino S, Guelpa E, Melli R, Sciacovelli A, Sciubba E, Toro C, Verda V, Optimal operation and sensitivity analysis of a large district heating network through POD modeling. Proceedings of International Mechanical Engineering Congress & Exposition; 2014 November 14-20; Montreal, Canada.

[31] Guelpa E, Barbero G, Sciacovelli A, Verda V. Thermal load peak shaving in district heating systems through optimization of users request.Proceedings of Ecos 2016 - The 29th International Conference on Efficiency, Cost, Optimization, Simulation and environmental impact of energy systems, June 19-23, 2016, Portorož, Slovenia.

[32] Verda V, Guelpa E, Sciacovelli A, Acquaviva A, Patti E. Thermal peak load shaving through users request variations. International Journal of Thermodynamics 2016; 19(3): 168-176.

[33] Verda, V, Caccin M, Kona A. Thermoeconomic cost assessment in future district heating networks. Energy 2016; 117(2): 485–491.

NOMENCLATURE

A: incidence matrix
b: branches number
c: specific heat, J/(kg K)
D: pipe diameter, m
f: distributed friction factor
G: mass flow rate, kg/s
k: thermal conductivity W/(mK)
K: stiffness matrix
L: loop number
L: pipe length, m
M: mass matrix, kg
n: node number
p: pressure, Pa
P: pressure matrix, Pa
R: residual
S: subsystem number
S: pipe section, m2
T: time, s
T: temperature, _C
U: pipe transmittance, W/kg K

V: volume, m3
Y: fluid dynamic conductance

Greek symbols
α: under-relaxation factor
β: localized friction factor
ρ: density, kg/m3
τ: pumping pressure vector, Pa
φ: heat losses, W
Φ: heat power W

Subscripts and superscripts
corr: correction
env: environmental
ext: external
in: inlet
out: output
RET: return
SUP: supply

LIST OF TABLES

LIST OF FIGURES

TABLES

Plant	Type	Nominal Power [MW]
Torino Nord	Cogeneration	220
	Boilers	340
	Storage	150
Moncalieri	2 Cogeneration plants	520
	Boilers	141
Politecnico	Boilers	255

	Storage	60
Martinetto	Storage	60
BIT	Boilers	255
Mirafiori Nord	Boilers	35

Table 2 Characteristics of the thermal plants

		U1		U2		U3		U4	
		h	*min*	*h*	*min*	*h*	*min*	*h*	*min*
1	*on*	6	10	5	15	3	45	5	15
	off	22	10	22	15	9	45	14	5
2	*on*					10	15	15	30
	off					13	45	22	5
3	*on*					14	20		
	off					21	45		

Table 2 Heating systems time schedules

FIGURES

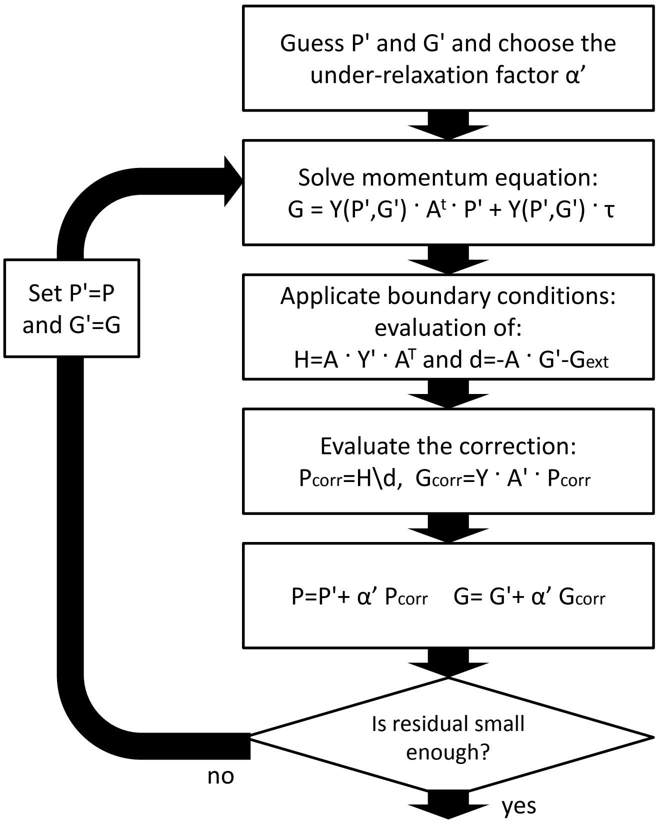

Figure 1. Schematic of the SIMPLE procedure

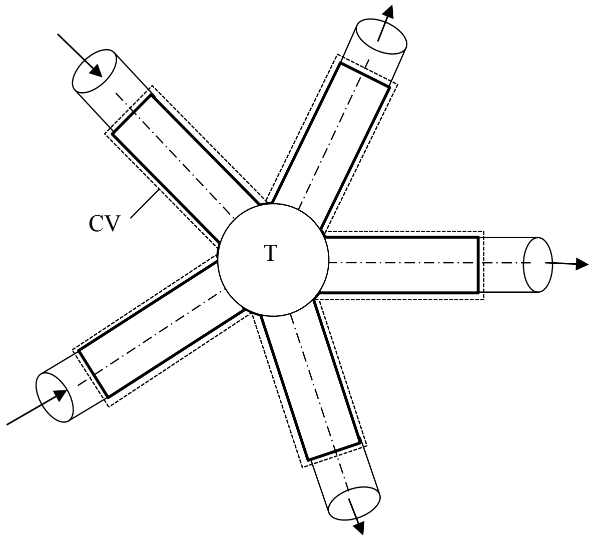

Figure 2. Schematic of the control volume of a node

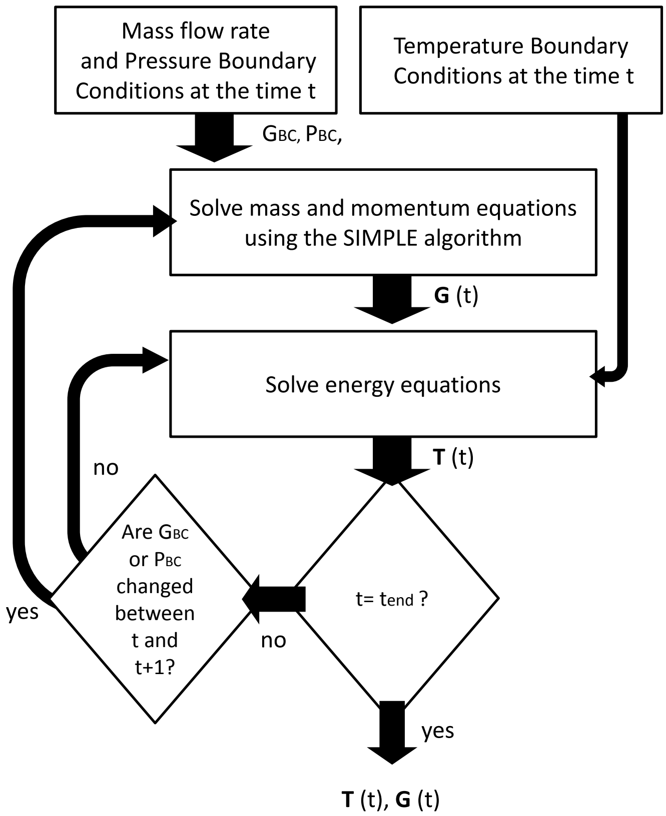

Figure 3. Schematic of procedure used to solve the thermal fluid dynamic problem

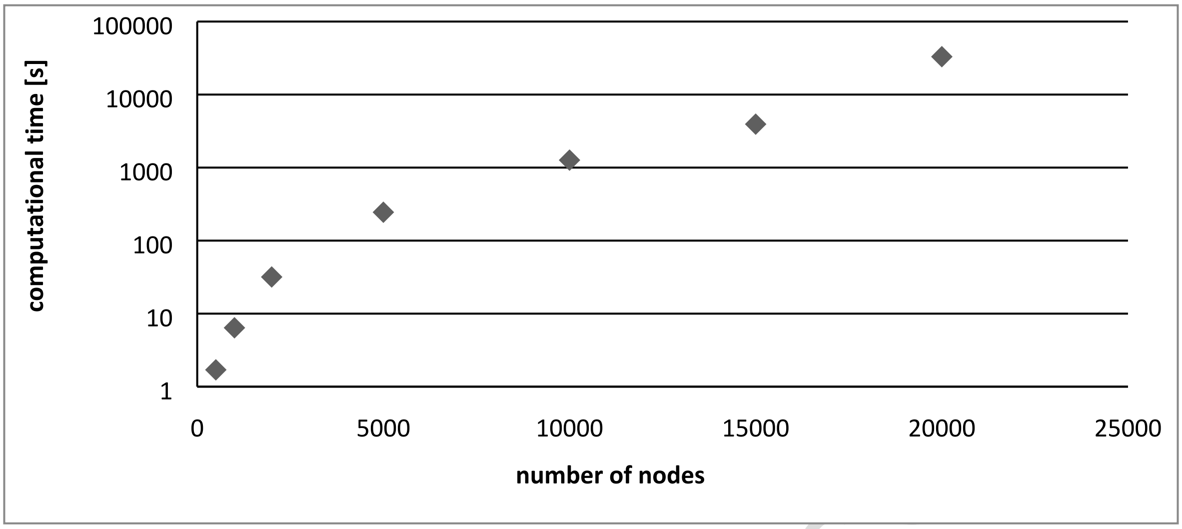

Figure 4. Computational time to solve the thermo-fluid dynamic model as the function of the number of nodes

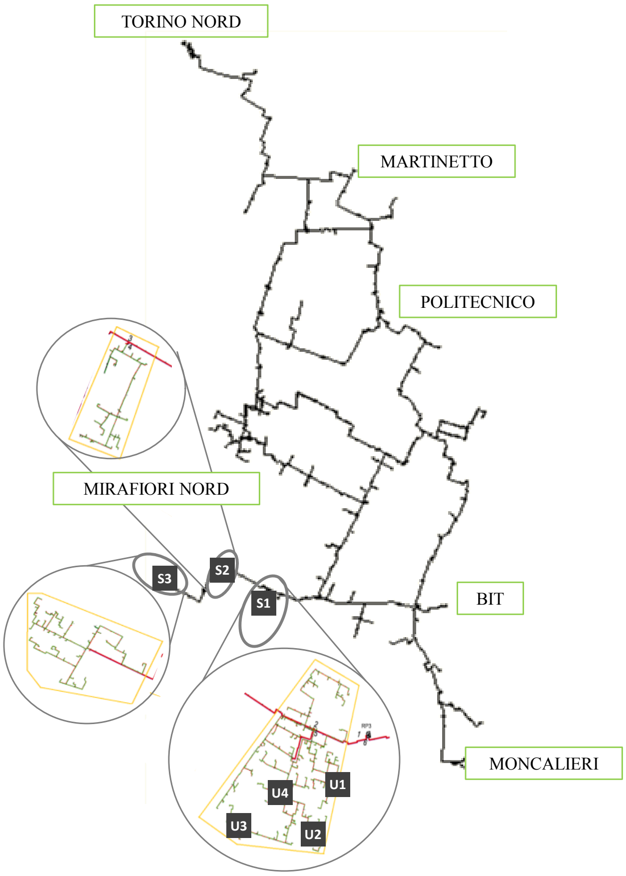

Figure 5 Schematic of Turin District Heating Network. In evidence three distribution networks and the thermal plants

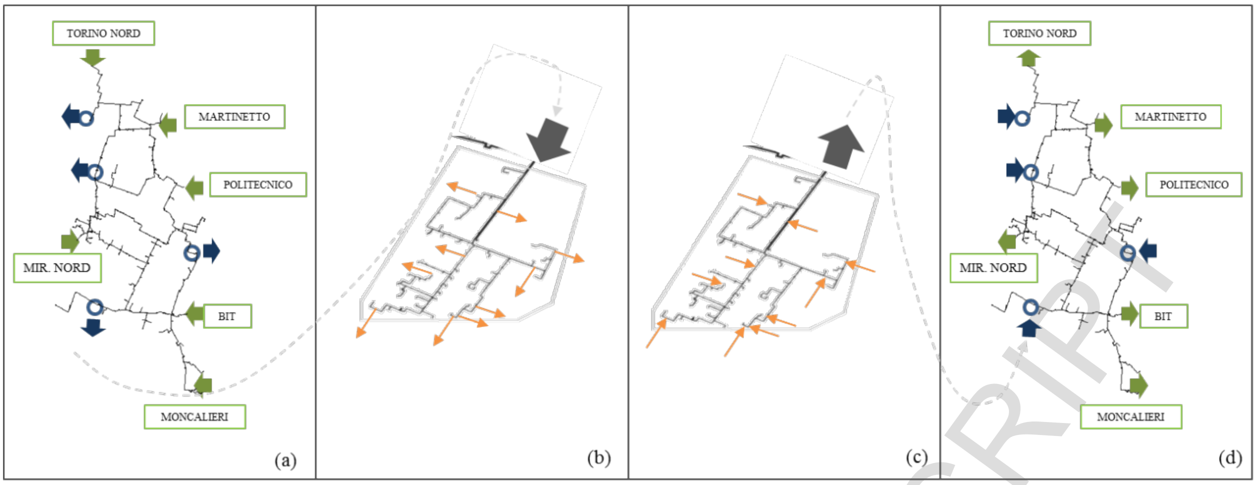

Figure 6 Schematic of the approach for the network modelling

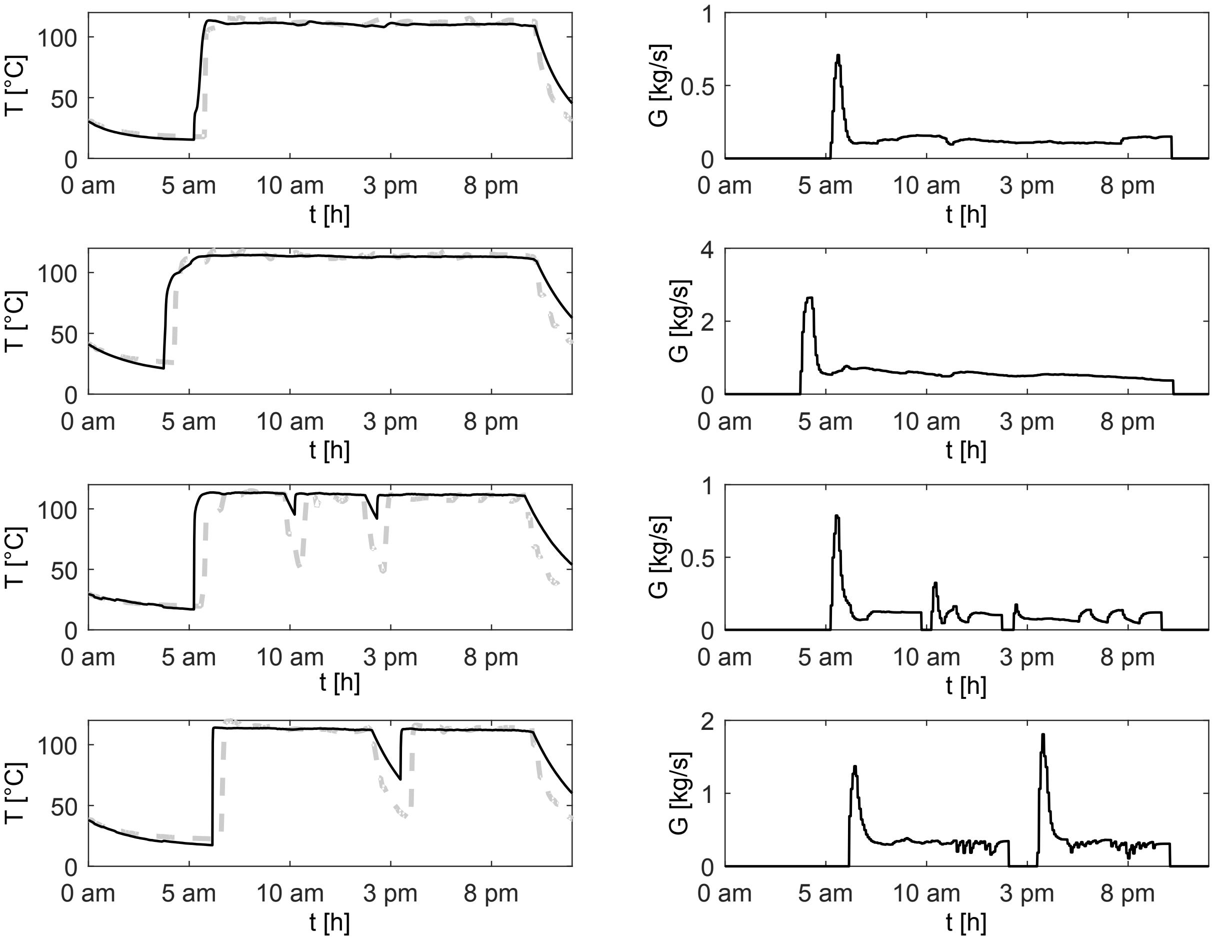

Figure 7. Temperature and mass flow rate, respectively from the top down at the inlet section of U1, U2, U3 and U4 heat exchangers: dashed line= experimental data, solid line=model results

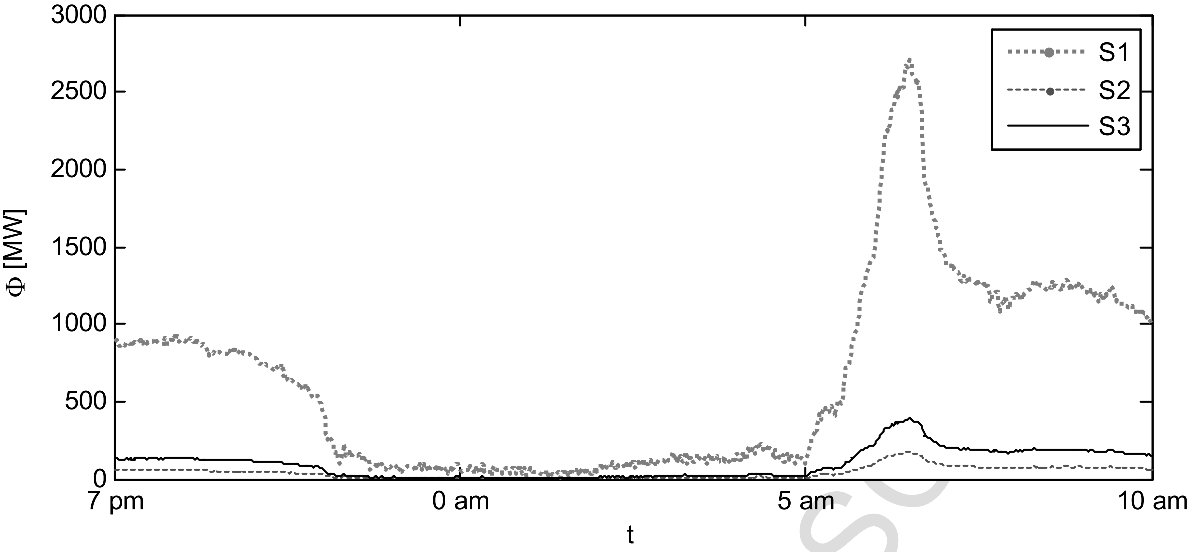

Figure 8. Thermal request at the barycentres S1, S2, S3

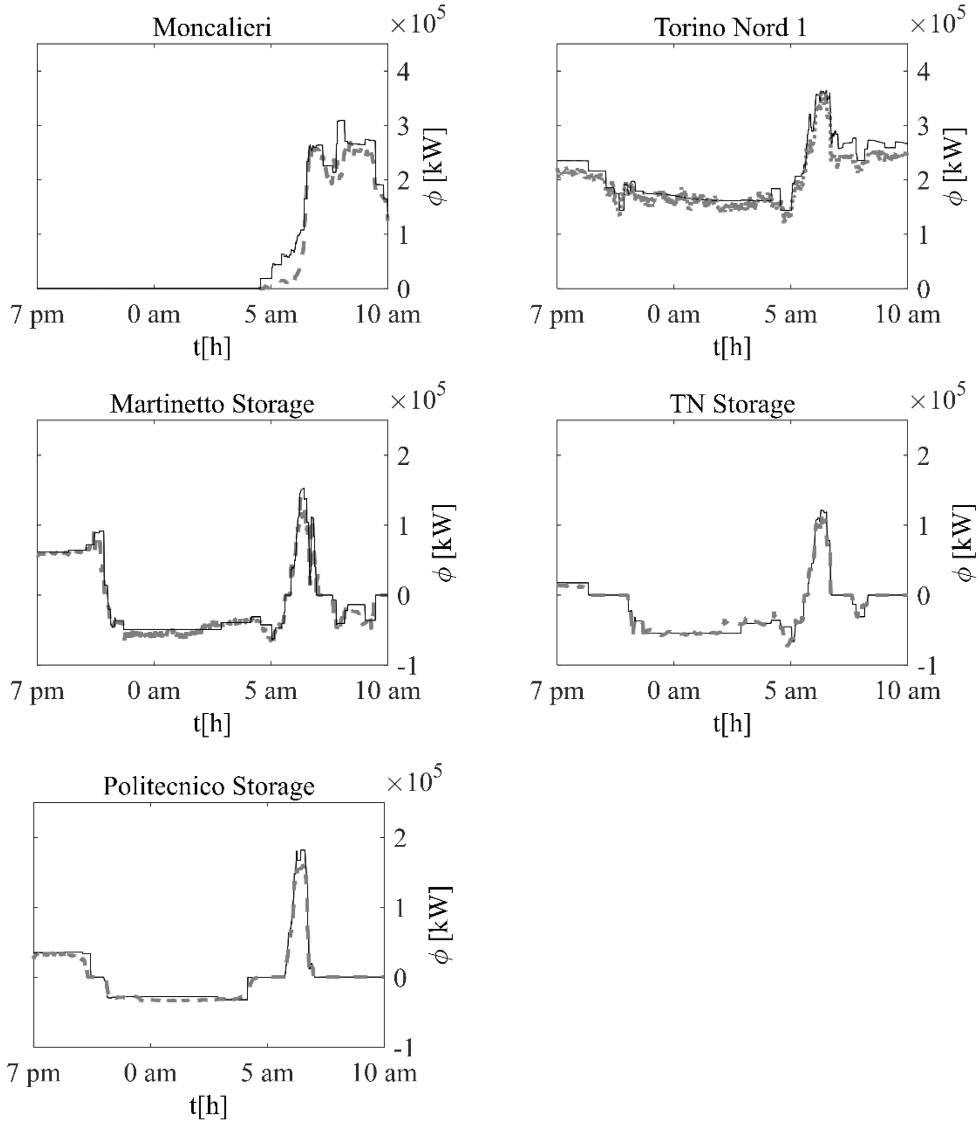

Figure 9. Heat Flux evolution at the thermal plants (Black line: simulation, grey dashed line: measurements)

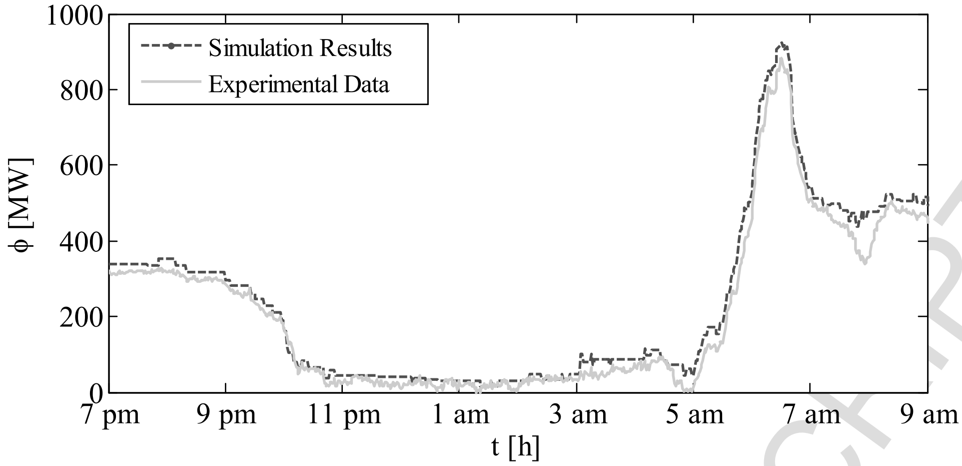

Figure 10. Total heat power evolution during the night transient. Comparison between real data and simulation results.

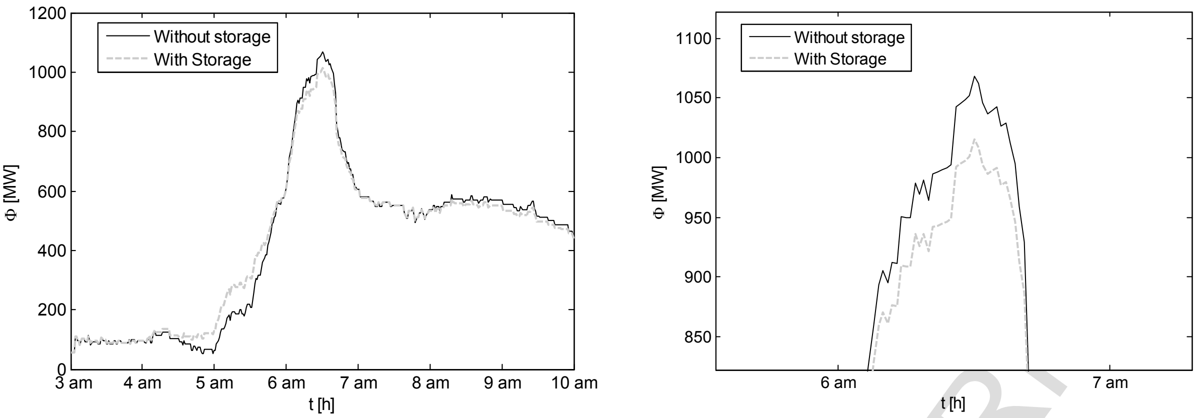

Figure 11. Thermal load after the inclusion of the new area. a) All the transient b) Peak comparison

A thermo-fluid dynamic model for the detailed simulation of large DHNs is proposed

The model receives data from the substations as the input

The transient simulation of the Turin DHN is compared with measurements

The model can be applied to implement advanced management strategies